Physics of Semiconductors. Phase equilibria and phase transitions

UDC 538.9

EDN QMUSSM
https://www.doi.org/10.33910/2687-153X-2023-4-3-131-138

Admittance of AgI films in the temperature range of the semiconductor-superionic phase transition

A. V. Ilinskiy[1], R. A. Castro Arata[2], V. A. Klimov[1], A. A. Kononov[2], M. E. Pashkevich[3], I. O. Popova[2], E. B. Shadrin[✉1]

[1] Ioffe Physical-Technical Institute, 26 Politekhnicheskaya Str., Saint Petersburg 194021, Russia
[2] Herzen State Pedagogical University of Russia, 48 Moika Emb., Saint Petersburg 191186, Russia
[3] Peter the Great Saint Petersburg Polytechnic University, 29 Politekhnicheskaya Str., Saint Petersburg 195251, Russia

Authors

Aleksandr V. Ilinskiy, ORCID: 0000-0002-1548-1180, e-mail: Ilinskiy@mail.ioffe.ru

Rene Alejandro Castro Arata, ORCID: 0000-0002-1902-5801, e-mail: recastro@mail.ru

Vladimir A. Klimov, ORCID: 0000-0002-9096-7594, e-mail: vlad.a.klimov@mail.ioffe.ru

Alexey A. Kononov, ORCID: 0000-0002-5553-3782, e-mail: kononov_aa@icloud.com

Marina E. Pashkevich, ORCID: 0000-0002-3373-4129, e-mail: marpash@yandex.ru

Irina O. Popova, ORCID: 0000-0002-0822-985X, e-mail: timof-ira@yandex.ru

Evgeniy B. Shadrin, ORCID: 0000-0002-1423-2852, e-mail: shadr.solid@mail.ioffe.ru

For citation: Ilinskiy, A. V., Castro Arata, R. A., Klimov, V. A., Kononov, A. A., Pashkevich, M. E., Popova, I. O., Shadrin, E. B. (2023) Admittance of AgI films in the temperature range of the semiconductor-superionic phase transition. *Physics of Complex Systems*, 4 (3), 131–138. https://www.doi.org/10.33910/2687-153X-2023-4-3-131-138 EDN QMUSSM

Received 13 June 2023; reviewed 5 July 2023; accepted 5 July 2023.

Funding: This study was supported by the Ministry of Education of the Russian Federation as part of the state-commissioned assignment (project No. VRFY-2023-0005).

Abstract. In the temperature range (80–250) °C, the frequency dependence of the admittance of thin (90 nm) AgI films with a semiconductor-superionic phase transition has been studied. The applicability of the Debye theory for modeling the physical mechanism of the dielectric response of a material to the action of an alternating electric field is shown. It has been found that the reported experimental technique makes it possible to separately determine the parameters of the electronic and ionic components of the electrical conductivity of a superionic.

Keywords: impedance, admittance, dielectric measurements, AgI, phase transition, superionic

Introduction

Dielectric spectroscopy is a method for obtaining the parameters of the electrical response of the material under study to the action of a low-frequency alternating electric field ($f \le 10^7$ Hz) (Kremer, Schonhals 2003).

The measured parameters are the frequency dependence of the current density $j(f)$ flowing through the cell of the dielectric spectrometer at voltage $\nu(f)$, as well as the angle between the voltage and current vectors.

For an ideal dielectric, the bias current leads the voltage in phase by an angle $\psi = \pi/2$ at any frequency. For a non-ideal dielectric, the angle ψ depends on the frequency and turns out to be smaller than $\pi/2$ by some amount $\delta(f) = \pi/2 - \psi(f)$ (Sidorovich 1984).

The angle δ(f) is measured in degrees or radians. For the analysis, however, the dimensionless quantity tg$\delta(f)$ is usually used, which is equal to the ratio of the charge carrier drift current density to the bias current density flowing through the measuring cell of a dielectric spectrometer (Macdonald 2006).

The drift current is accompanied by energy losses. It follows from this that the smaller the angle $\delta(f)$, the lower the energy loss. Therefore, the value of tg$\delta(f)$ is positioned as the tangent of the dielectric loss angle (Fröhlich 1958).

Recently, dielectric spectroscopy has been rapidly developed in connection with the creation of industrial dielectric spectrometers with high sensitivity, equipped with high-speed computers with modern software (Egorov et al. 2018). Spectrometers calculate a large number of dielectric parameters based on $j(f)$ and tg$\delta(f)$. Namely, the frequency dependences of the complex permittivity $\varepsilon^*(f)$, complex resistance $z^*(f)$, complex conductivity $\sigma^*(f)$, electric capacitance of the cell, etc., are calculated. No new information arises when the spectra $\varepsilon^*(f)$ are rebuilt to the spectra $z^*(f)$ or $\sigma^*(f)$. But such a restructuring allows to choose a specific type of spectra. This choice is related to the convenience of interpreting the spectra. In this case, it becomes possible to build special functional dependencies. For example, excluding such a parameter as frequency f from the formulas allows you to construct a function $\varepsilon''(\varepsilon')$, called the Cole-Cole diagram, or $z''(z')$, called the impedance, or $\sigma''(\sigma')$, called the admittance of the substance under study. Such dependences do not contain new information, either. Instead, they clarify specific features of the registered dielectric spectra.

This article explores the mechanism of the phase transition from the hexagonal β-phase to the cubic body-centered α-phase in thin AgI crystalline films. This transition occurs near the critical temperature of 147 ^{0}C and is a semiconductor-superionic phase transition. In the high-temperature α-phase in an external electric field, along with an increase in electronic conductivity, ionic conductivity arises. Ionic conductivity is due to the partial "melting" of the silver sublattice and the abrupt motion of silver ions along the direction of the external electric field. It turned out that these processes are clearly manifested in the dielectric spectra. The article reports and analyses the results of the study.

Experimental technique

AgI samples

We synthesized 95 nm thick nanocrystalline AgI films on 40 μm thick optical mica substrates. The first phase of synthesis was thermal deposition of an 80 nm thick layer of metallic silver on a mica substrate. At the next phase of the synthesis, thermal iodination of metallic silver was performed according to the Ag + I = AgI reaction. The mica temperature stabilized at T = 150 ^{0}C, and crystalline iodine was sublimated at T = 110 ^{0}C.

Dielectric measurements

Dielectric measurements were carried out with Concept 81 (Novocontrol Technologies GmbH & Co. KG, Montabaur, Germany; "Modern physical and chemical methods of formation and study of materials for the needs of industry, science and education", Herzen University). The film under study was placed in the measuring device of the spectrometer, made in the form of a flat capacitor. The region of frequency variation corresponded to the range $f = (10^{-1} \div 10^7)$ Hz.

The frequency spectra were studied at fixed temperatures, which varied with a step of 10 ^{0}C in the range of (80–250) ^{0}C.

In this case, the frequency dependences of the real $\sigma'(f)$ and imaginary $\sigma''(f)$ parts of the complex electrical conductivity σ^* of the sample were recorded separately. For the convenience of analysis, the results of the experimental determination of $\sigma'(f)$ and $\sigma''(f)$ were presented as the admittance $\sigma''(\sigma')$ of the AgI films. In addition, the frequency dependences of the dielectric loss tangent tgδ (f) were recorded.

Since the AgI film is studied together with the substrate by the dielectric method, we performed a separate measurement of the conductivity of mica free of the AgI film. It turned out that the value of the specific conductivity of mica is small (< 10^{-15} S/cm) and does not depend on the frequency of the electric field. It is independent of the sample temperature, either. Consequently, the obtained results characterize only the AgI film.

When analyzing the results of dielectric measurements, we proceeded from the fact that the electrical response of the sample is linear if a sinusoidal voltage of frequency ω and amplitude U_o is applied to the measuring cell. The linearity of the response makes it possible to apply the symbolic calculation

 https://www.doi.org/10.33910/2687-153X-2023-4-3-131-138

method, when the frequency dependences of current and voltage are presented in a complex form (Tolstykh, Gozbenko 2010):

$$U(t) = U_0 \sin(\omega t) = Im\left[U^* \exp(i\omega t)\right], \quad (1)$$

$$I(t) = I_0 \sin(\omega t + \phi) = Im\left[I^* \exp(i\omega t)\right], \quad (2)$$

where the symbols U^* and I^* represent the complex voltage and current amplitudes, respectively. We set $U^* = U_0$ and extract explicitly the real and imaginary parts of complex quantities. Therefore, we can write $I^* = I_0 \exp(i\phi) = I_0 \cos(\phi) + iI_0 \sin(\phi)$, where $I_0 = (I' + I'')^{1/2}$, and i is the imaginary unit. From the complex form of Ohm's law $I^*(t) = U^*(t)/Z^*$ we obtain $Z^* = [U_0 \exp(i\omega t)]/[I^* \exp(i\omega t)]$, that is $(Z' + iZ'') = \dfrac{U_0}{I' + iI''}$ or $Z' = (U_0/I_0)I'$ and $Z'' = (U_0/I_0)I''$.

The design of the dielectric spectrometer makes it possible to measure the real amplitudes U_0 and I_0, as well as the tangent of the angle between the total impedance vector of the sample and the real axis. This angle coincides with the angle ϕ of the phase difference between current fluctuations through the sample and voltage fluctuations applied to the sample. That's why $tg\delta = I''/I'$. Given expressions $Z' = (U_0/I_0)I'$ and $Z'' = (U_0/I_0)I''$, we get $tg\delta = Z''/Z'$.

As mentioned above $I_0 = (I')^2 + (I'')^2$ and $tg\delta = I''/I'$. Thus, we get $I' = I_0/[1 + (tg\phi)^2]^{-1/2}$ and $I'' = (I_0 tg\phi)/[1 + (tg\phi)^2]^{-1/2})$, where I_0 and ϕ are experimental values measured by the spectrometer for each frequency $\omega = 2\pi f$ of input voltage fluctuations. The frequency f varies in the range $f = 10^1 - 10^6$ Hz. This allows us to experimentally determine the real and imaginary parts of the complex impedance Z^* according to the expressions $Z' = (U_0/I_0)I'$ and $Z'' = (U_0/I_0)I''$.

The design of the measuring cell of the spectrometer is such that the inductive component of the total impedance of the film sample is negligibly small. It follows from this that when analyzing the frequency dependence of the reactive component of the complex impedance Z^*, only the complex electrical capacitance C^* of the measuring cell with the sample should be taken into account. Therefore, the complex permittivity of the sample $\varepsilon^* = \varepsilon' + i\varepsilon''$ is introduced into consideration, which is obtained from the relationship $Z^* = 1/(i\omega C^*) = 1/(i\omega C_0 \varepsilon^*)$. After that, simple calculations lead to the expression $\varepsilon' + i\varepsilon'' = 1/(\omega C_0 Z'' + i\omega C_0 Z')$. Getting rid of the imaginary in the denominator and equating to each other the real and imaginary parts of ε^*, we obtain the relations:

$$\varepsilon' = -Z''/\left\{\omega C_0\left[\langle Z''\rangle^2 + \langle Z'\rangle^2\right]\right\}, \quad (3)$$

$$\varepsilon'' = -Z''/\left\{\omega C_0\left[\langle Z''\rangle^2 + \langle Z'\rangle^2\right]\right\}, \quad (4)$$

where Z' and Z'' are the real and imaginary parts of the complex impedance of the sample, thus determined for each frequency ω of input voltage oscillations.

Taking into account expressions $Z' = (U_0/I_0)I'$ и $Z'' = -(U_0/I_0)I''$ and expressions $I' = I_0/[1 + (tg\phi)^2]^{-1/2}$ and $I'' = (I_0 tg\phi)/[1+(tg\phi)^2]^{-1/2}$, we get a connection between ε', ε'' and measured quantities I_0, U_0 and ϕ:

$$|\varepsilon'| = (I_0 tg\phi)/\left[\omega C_0 U_0\left(1 + (tg\phi)^2\right)^{-1/2}\right], \quad (5)$$

$$|\varepsilon''| = I_0/\left[\omega C_0 U_0\left(1 + (tg\phi)^2\right)^{-1/2}\right]. \quad (6)$$

The use of the general formulas of complex analysis (Krantz et al. 1999) allows us to proceed to obtain the real part $\sigma'(f)$ and the imaginary part $\sigma''(f)$ of the specific conductivity.

Experimental results

Fig. 1 shows the frequency spectra of the real part $\sigma'(f)$ (a) and the imaginary part $\sigma''(f)$ (b) of the specific conductivity of the spectrometer cell with the AgI film. The measurements were carried out at fixed temperatures near b→α phase transition (140 °C < T < 167 °C). In this case, the measurements

were carried out with a step of 3 ^{0}C. At the first stage, the sample was heated from 140 ^{0}C to 167 ^{0}C, and then cooled to 140 ^{0}C in order to register a thermal hysteresis loop. In addition, with a wider step equal to 10 ^{0}C, the dielectric spectra of the AgI film were measured at higher temperatures of up to 250 ^{0}C.

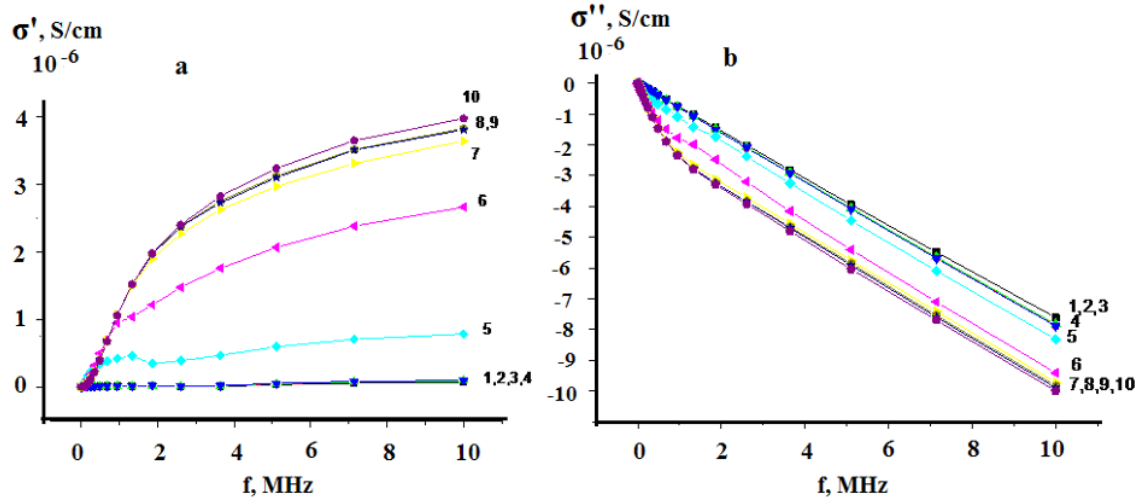

Fig. 1. Frequency dependences of the real $\sigma'(f)$ and imaginary $\sigma''(f)$ parts (b) of the specific conductivity of a spectrometer cell containing a sample of silver iodide (AgI). 1—140, 2—143, 3—146, 4—149, 5—152, 6—155, 7—158, 8—161, 9—164, 10—167 ^{0}C

Fig. 1a shows the dependence of the spectra $\sigma'(f)$ on temperature (curves 1–10). The strongest dependence was observed near the temperature b→α phase transition (curves 4–7). It turned out that the specific conductivity $\sigma'(f)$ has the highest value at high frequencies (f = 1 GHz). The imaginary part of the conductivity $\sigma''(f)$ at frequencies f > 1 MHz linearly increases in absolute value with increasing frequency (Fig. 1b). At low frequencies (f→0) the imaginary part tends to 0 ($\sigma''(f)$→0 at f→0). However, in Fig. 1a, the features of the spectra $\sigma'(f)$ at low and medium frequencies are not clearly visible. Therefore, for the convenience of analysis, these spectra are presented in Fig. 2 on a double logarithmic scale. Fig. 2 shows that the graphs of the functions $s'(f)$ at medium frequencies have a complex shape. Since the reason for the mutual intersection at frequency f = 104 Hz of the graphs of the functions $\sigma'(f)$ recorded at different temperatures remains unclear, the analysis of the results of these experiments requires additional research.

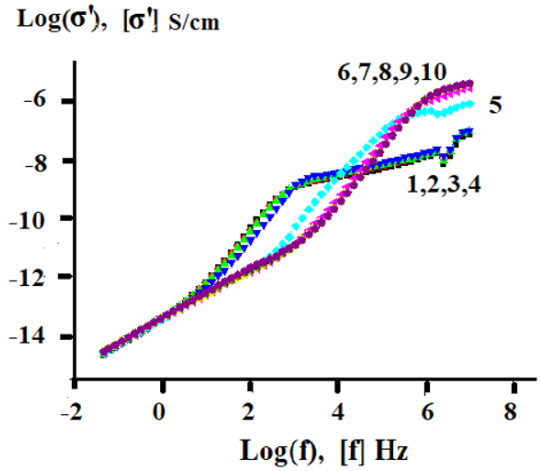

Fig. 2. Log-log frequency dependence of the real $\sigma'(f)$ part of the conductivity of a spectrometer cell containing a sample of silver iodide (AgI). 1—140, 2—143, 3—146, 4—149, 5—152, 6—155, 7—158, 8—161, 9—164, 10—167 ^{0}C

 https://www.doi.org/10.33910/2687-153X-2023-4-3-131-138

To facilitate the analysis of the dielectric spectra, we performed their rearrangement in the form of Cole-Cole diagrams $\varepsilon''(\varepsilon')$, complex impedance $Z''(Z')$ and complex conductivity admittance $\sigma''(\sigma')$. Fig. 3 shows a graph of the complex admittance, that is, the dependence of the imaginary part of the conductivity σ'' on its real part σ'.

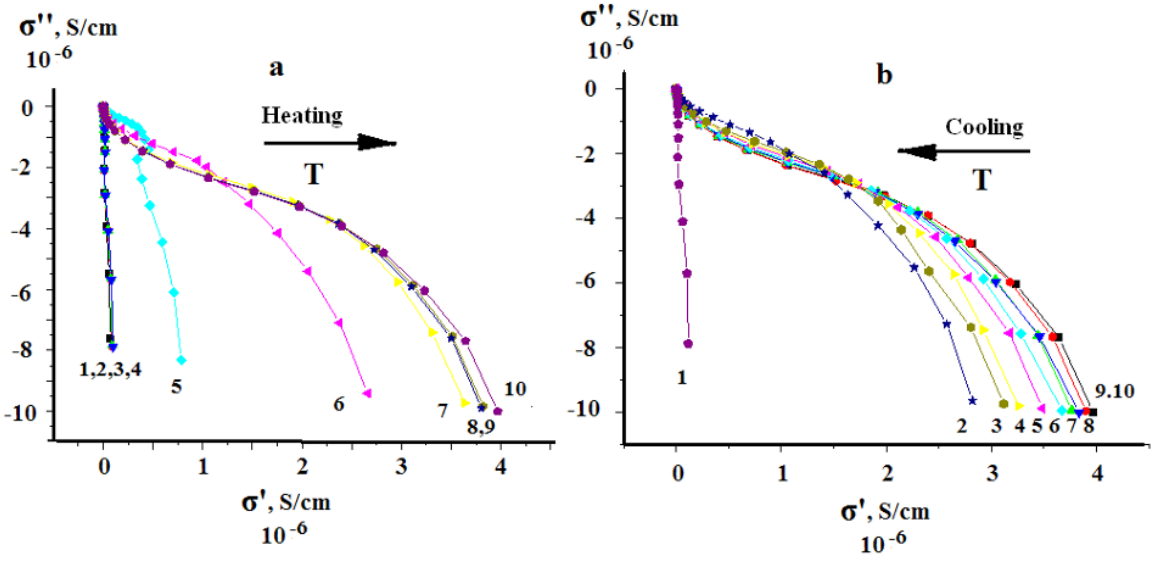

Fig. 3. Admittance $s''(s')$ of the specific conductivity of a spectrometer cell containing a silver iodide (AgI) sample in the temperature range of 140–167 0C: a—heating, b—cooling. 1—140, 2—143, 3—146, 4—149, 5—152, 6—155, 7—158, 8—161, 9—164, 10—167 ^{0}C

Fig. 4a shows the frequency dependences of the dielectric loss tangent $\mathrm{tg}\delta(f)$ in a wide temperature range (80 < T < 240 ^{0}C).

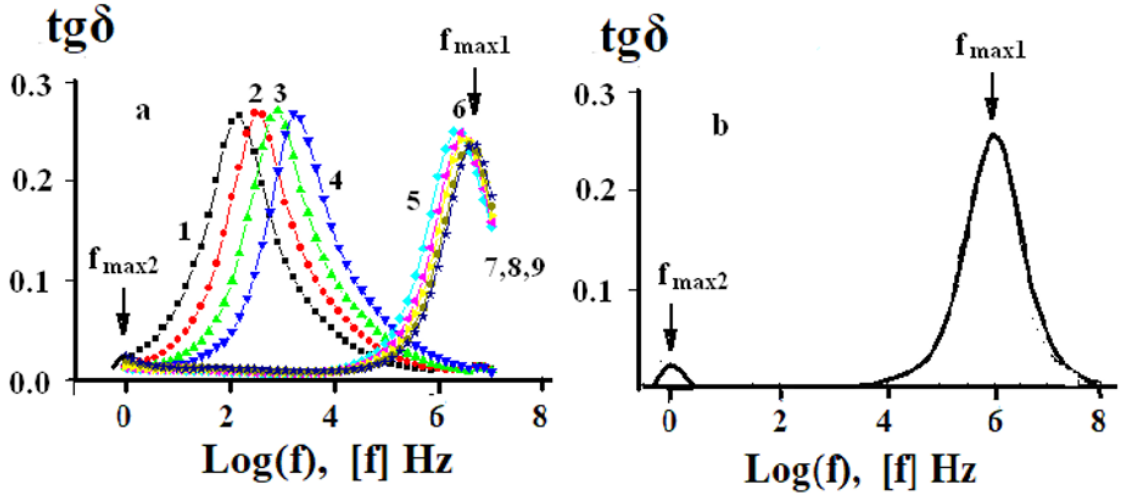

Fig. 4. Frequency dependences of the dielectric loss tangent $\mathrm{tg}\delta(f)$: a) experiment for T = 80 – 240 ^{0}C (1—80, 2—100, 3—120, 4—140, 5—160, 6—180, 7—200, 8—220, 9—240 ^{0}C), b) calculation with formula $\mathrm{tg}\delta(f) = \varepsilon''(f)/\varepsilon'(f)$ for T = 240 ^{0}C

Admittance $\sigma''(\sigma')$ of AgI films in the temperature range of 140–160 ^{0}C is a system of graphs approaching the real axis σ' at high frequencies (Fig. 3a—heating, Fig. 3b—cooling). Fig. 3 shows the difference in the graphs of the functions $\sigma''(\sigma')$ for different temperatures. Extrapolation of the graphs to the real axis σ' ($f\to\infty$) makes it possible to determine the specific conductivity σ(T) of the AgI film for different temperatures. Note that the admittance of silver iodide films $\sigma''(\sigma')$ at high temperatures T = (200, 210, 220, 230, 240, 250) ^{0}C reveals an additional feature at low frequencies (Fig. 5).

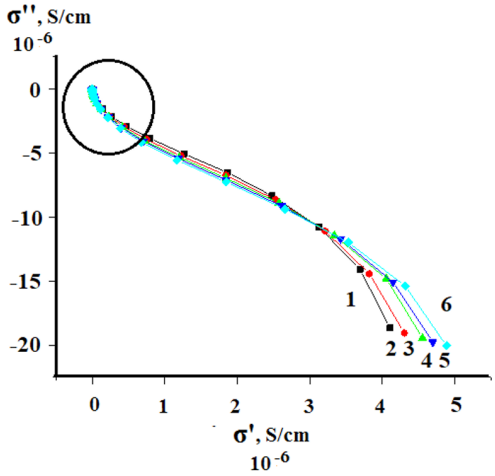

Fig. 5. Admittance *s*”(*s*’) of the specific conductivity of a spectrometer cell containing a sample of silver iodide (AgI), in the temperature range 210–250 ^{0}C. (1—210, 2—220, 3—230, 4—240, 5—250 ^{0}C)

The spectrum tg$\delta(f)$ (Fig. 4a) has a maximum at the frequency f_{max1} corresponding to the relaxation time $\tau_1 = 1/2\pi f_1$. The position of the maximum of the function tg$\delta(f)$ depends on the temperature and is located at the frequency f_{max1} =100 Hz at T = 80 ^{o}C. Its absolute value is tg$\delta(f_{max1})$ = 0.27. As the temperature increases, this maximum shifts towards higher frequencies without changing the absolute value. In the temperature range of 140–160 ^{0}C (curves 4,5, Fig. 4a) there is an abrupt increase in the frequency position of this maximum. With further heating (up to 240 ^{0}C), a second weak maximum tg$\delta(f)$ appears in the low-frequency region (curves 8, 9). It is located at the frequency f_{max2} = 1 Hz. Consequently, the spectral dependence tg$\delta(f)$ at high temperatures is characterized by two relaxation times: τ_1(T) and τ_2(T). When the spectrometer cell is cooled, the maximum tg$\delta(f)$ returns to its original positions, but with a temperature delay of 10 ^{0}C.

Fig. 6 shows thermal hysteresis loops for $f_{max1}(T)$, σ(T), and σ’(T). The values of σ(T) are determined from the frequency position f_{max1} of the maximum of dielectric loss tangent using the formula $\tau_M = 1/(2\pi f_1)$. This uses the definition of the Maxwellian relaxation time in the form $t_M = ee_o/\sigma$. The specific conductivity σ (T) of the AgI film is determined from Fig. 3 by extrapolating the imaginary part σ” to the real axis σ’. The loop width is taken to be the temperature difference corresponding to those points of the heating and cooling branches of the loop, which are located at half the height of the frequency jump. The experiment showed that the widths of all three loops are equal to 10 ^{0}C. The shape and height of the loops also coincide (Figs. 6b and 6c) within experimental errors (5%).

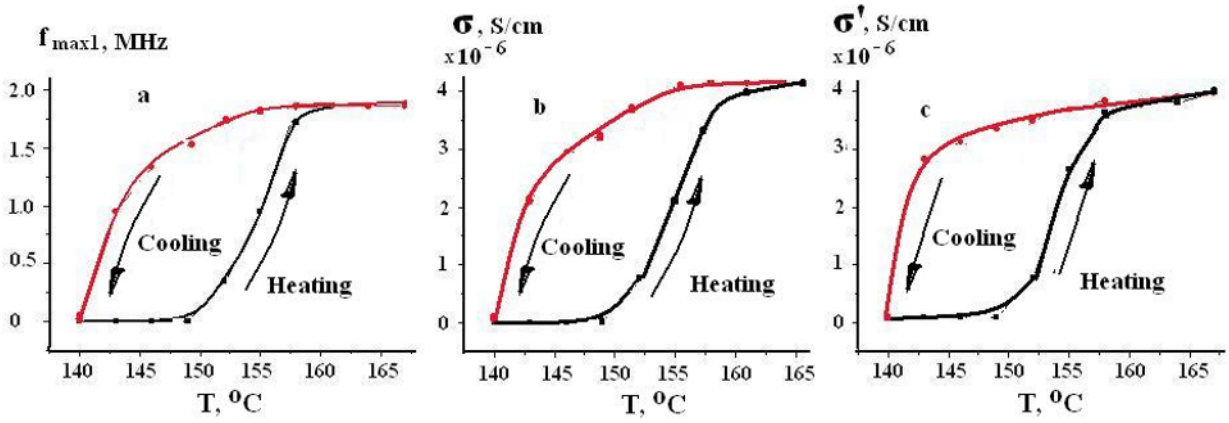

Fig. 6. Temperature hysteresis loops. Fig. 6a. Frequency position f_1 of maximum 1 dielectric loss tangent;
Fig. 6b. Conductivity σ of an AgI film, determined from Fig. 6a using the formula $\sigma_M = ee_o/\tau_M = ee_o \times 2\pi f$;
Fig. 6c. Conductivity σ’ of the AgI film, determined from Fig. 3 by extrapolation of the imaginary part σ” to the real axis σ’

 https://www.doi.org/10.33910/2687-153X-2023-4-3-131-138

Calculation results

Creating a model of the reaction mechanism of a thin film of silver iodide to an applied low-frequency sinusoidal electric field requires the calculation of the functions $\varepsilon'(f)$ and $\varepsilon''(f)$. In the reported study, this calculation was carried out on the basis of the Debye theory. After performing the calculation, the frequency dependence of the function $\mathrm{tg}\delta(f) = \varepsilon''(f)/\varepsilon'(\mathrm{f})$ was plotted.

The calculations are performed for a system with two types of relaxators with relaxation times τ_1 and τ_2. This kind of model of a relaxing system makes it possible to apply the expression for $\varepsilon^*(\omega)$ in the form

$$\varepsilon^*(\omega) = \varepsilon_\infty + \frac{\Delta\varepsilon_1}{1+(i\omega\tau_1)} + \frac{\Delta\varepsilon_2}{1+(i\omega\tau_2)}\ , \tag{7}$$

ε_∞—high-frequency limit of the real part of the permittivity ε^*, $\Delta\varepsilon_1$ и $\Delta\varepsilon_2$—jumps in the real part ε^*, $\omega = 2\pi f$—cyclic frequency.

Fig. 4b reproduces on a logarithmic scale the graphical representation of the function $\mathrm{tg}\delta(f) = \varepsilon''/\varepsilon'$ based on expression (7). Dependence $\mathrm{tg}\delta(f)$ has two maxima at frequencies $f_{\max1}$ and $f_{\max2}$. The parameters of formula (7) correspond to experimental data at T = 240 °C. At this temperature, the high-frequency and low-frequency features of the DS are clearly expressed in the experiment. Comparison of plots of experimental (Fig. 4a, curve 9) and calculated functions $\mathrm{tg}\delta(\mathrm{f}) = \varepsilon''/\varepsilon'$ (Fig. 4b) confirms the applicability of the Debye theory for a qualitative explanation of the shape of the experimental dielectric spectra of AgI (Figs. 1–3).

Results and discussion

According to our model, the experimental features of the function $\mathrm{tg}\delta(f)$ are determined by the physical properties of the relaxators. Specifically, high frequency features are determined by free electrons; low frequency features are determined by positively charged free silver ions. The relaxation times in this model coincide with the Maxwellian relaxation times $\tau_M = \varepsilon\varepsilon_o/\sigma$. Here, σ is the electrical conductivity of the material.

The expression for the Maxwellian relaxation time makes it possible to transform the thermal hysteresis loop $f_{\max1}(T)$ (Fig. 6a) into the hysteresis loop of the electrical conductivity $\sigma(\mathrm{T})$ of the crystal (Fig. 6b). Comparison of the characteristics of the hysteresis loops of electrical conductivity (Fig. 6b and Fig. 6c) shows the qualitative and quantitative agreement of these characteristics. Loop parameters (Fig. 6c) were obtained by calculating the electrical admittance of the AgI films (Fig. 3). The obtained agreement confirms the legitimacy of using the concept of Maxwellian relaxation time for analysis.

For free silver ions at T = 240 °C the Maxwellian relaxation time is very long $\tau_{M2} = 1.6 \times 10^{-1}$ s ($f_{\max2}$ = 1 Hz—line 9, Fig. 4a).

At T=80 °C, that is, away from temperatures g→β and b→α phase transitions, the Maxwellian relaxation time is large: τ_{M1}=1.6 × 10^{-3} s ($f_{\max1} = 10^3$ Hz and $f_{\max1} = 10^6$ Hz—lines 4, 5, Fig. 4a), 150 °C Maxwellian time decreases by several orders to $\tau_{M1} = 1.6 \times 10^{-7}$ s near these phase transitions at T = (140 ÷ 150) °C.

The difference of several orders of magnitude between the Maxwellian relaxation times of free electrons and free silver ions is due to the fact that the electrical conductivity of the material is due to two types of free charge carriers. It is expressed by the formula $\sigma = en_e\mu_e + qn_q\mu_q$, where e and q are the charges of the electron and silver ion, while n_e, n_q and m_e, m_q are their concentration and drift mobility, respectively. The difference in the numerical values is due to the large difference in the drift mobilities of free electrons and ions.

An increase in the rate of thermal generation of free electrons reduces the Maxwellian relaxation time and shifts the maxima of the function $\mathrm{tg}\delta(f)$ in the direction of increasing frequency. In addition, at a temperature higher than the a→β phase transition temperature, quasi-free silver ions appear. Therefore, the electrical conductivity of the AgI crystal acquires an additional ionic character. Consequently, the strong difference in the frequency position of the maxima of the function $\mathrm{tg}\delta(f)$ confirms the possibility of using the dielectric spectroscopy method to separately study electronic and ionic processes in superionics.

Due to the above reasons the integrity of the superionic crystal is preserved despite the presence of free silver ions, which provide the ionic conductivity of the superionic.

For the α-phase, both the Ag+ ion and the I^- ion are at the centers of the cubes of their Bravais lattices. Each of the ions forms eight hybrid orbitals capable of forming seven low-strength donor-acceptor (coordination) bonds and one high-strength sigma bond. We are talking about the bonds between ions of opposite sign located at the corners of the cube of the Bravais lattices. In this case, the Ag atom donates only one electron taken from the $5s^1$ atomic orbital to eight hybrid orbitals. To create hybrid orbitals, he gives away seven of his empty $4f^0$ orbitals. Atom I, on the contrary, gives 15 electrons to eight hybrid orbitals.

Namely, it donates one electron from the $5p_z^1$ atomic orbital and 14 electrons from the rest of the orbitals participating in the hybridization. Thus, for eight Ag-I sigma bonds, there are, as required by the theory, a total of 16 electrons. But since the Ag atom donates only one electron, out of eight bonds, only one bond turns out to be a high-strength sigma bond of the usual type. This bond is formed by introducing into it one electron from each of the Ag^+ and I^- ions. The remaining seven electron-free $4f^0$ orbitals of the Ag ion receive 14 electrons donated by the I atom. Therefore, the remaining seven bonds turn out to be low-strength donor-acceptor bonds. At the same time, inside the ion-conducting channels, along which quasi-free Ag^+ ions move, all eight bonds are low-strength coordination bonds.

Thus, the obtained results show that drift ionic conduction arises in the α-phase of an AgI crystal in an external electric field. This conductivity arises due to directed jumps of "mobile" silver ions between crystal cells located along ion-conducting channels (see Fig. 7).

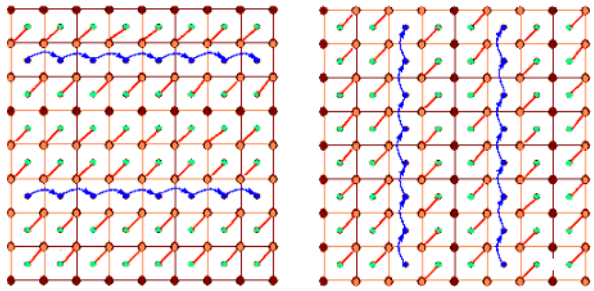

Fig. 7. Schematic representation of polytypes and ion-conducting channels

Conflict of Interest

The authors declare that there is no conflict of interest, either existing or potential.

Author Contributions

All the authors discussed the final work and took an equal part in writing the article.

References

Egorov, N. V., Karpov, A. G., Yanovskiy, V. V. (2018) Sistema issledovaniya dielektricheskikh materialov s pomoshch'yu shirokopolosnoj dielektricheskoj spektrometrii [System for research of dielectric materials by broadband dielectric spectrometry]. *Izvestiya SPbGETU "LETI" — Proceedings of Saint Petersburg Electrotechnical University*, 7, 31–37. (In Russian)

Fröhlich, H. (1958) *Teoriya dielektrikov [Theory of dielectrics]*. Moscow: "Izdatel'stvo inostr. lit." Publ., 341 p. (In Russian)

Krantz, S. G., Kress, S., Kress, R. (1999) *handbook of complex variables*. Boston: Birkhäuser Publ., 792 p. (In English)

Kremer, K., Schonhals, A. (2003) *Broadband dielectric spectroscopy*. Berlin: Springer Publ., 729 p. https://doi.org/10.1007/978-3-642-56120-7 (In English)

Macdonald, D. D. (2006) Reflections on the history of electrochemical impedance spectroscopy. *Electrochimica Acta*, 51 (8-9), 1376–1388. https://doi.org/10.1016/j.electacta.2005.02.107 (In English)

Sidorovich, A. M. (1984) Dielektricheskaya spektr vody [Dielectric spectrum of water]. *Ukrainskij fizicheskij zhurnal*, 29 (8), 1175–1181. (In Russian)

Tolstykh, O. D., Gozbenko, V. E. (2010) *Kompleksnye chisla [Complex numbers]*. Irkutsk: IrGUPS Publ., 64 p. (In Russian)